Performance Analysis of Frequency-Reconfigurable Antenna Cluster With Integrated Radio Transceivers

Jari-Matti Hannula, *Student Member, IEEE*, Marko Kosunen, *Member, IEEE*, Anu Lehtovuori, Kimmo Rasilainen, Kari Stadius, *Member, IEEE*, Jussi Ryynänen, *Senior Member, IEEE*, and Ville Viikari, *Senior Member, IEEE*

***Abstract*—A recently published antenna tuning concept promises efficient antenna performance over a wide bandwidth. The method relies on sophisticated control of phase and magnitude during reception and transmission. In this letter, we analyze the effect of tuning on the overall transceiver performance using simplified models for the transmitter and receiver. The results indicate the feasibility of the concept without significant effect on efficiency.**

***Index Terms*—Codesign, receiver, reconfigurable antenna, transmitter.**

I. Introduction

THE evolution of wireless communications challenges us to develop more versatile antenna–transceiver systems. The high data rates of future communications systems require wide frequency bands, and good impedance matching should be implemented over the entire frequency band to obtain high efficiency. The impedance interface between the antenna and the transmitter is challenging. Traditional antenna and integrated circuit design generally assumes that the impedance across the interface is 50 Ω. However, realizing this impedance is difficult for both the antenna and the transceiver electronics, forcing the designers to make compromises.

Traditionally, the antenna and the transceiver circuit are designed separately. Although there are some examples of antenna–transceiver codesign [1]–[4], the topic has not been significantly covered. Tunable solutions have been proposed both in the antenna and transceiver. Tuning has not been implemented using the antenna and the transceiver simultaneously.

A new concept for antenna design published in [5] and [6] relies on multiple antennas, which are mutually coupled and excited with different weights (signal amplitude and phase) to maximize the antenna efficiency. By adjusting the weights, a broad band can be covered with the same antenna structure. The results in [5] and [6] assume that the transceiver acts as an ideal 50 Ω interface to the antenna, and it can produce the required signals without loss of efficiency. However, this is not the case. For instance, a small weight corresponding to a low output power decreases power amplifier (PA) efficiency. Because of this, the benefit gained from using multiple antennas can be lost when the transmitter is used at inefficient power levels, reducing the total efficiency.

In this letter, we discuss the transceiver aspects of implementing the aforementioned antenna concept. We investigate the multiport antenna from [6]. We justify the use of specific architectures, demonstrate the effects of amplifier nonidealities on total efficiency, and obtain general guidelines on the operation of the antenna–transceiver system. For the transmitter, we use the efficiency model for an integrated outphasing PA [7]. The input impedance of the receiver front end is studied using both a simple, inductively degenerated amplifier model and a mixer-first receiver based on N-path filters.

The achieved results are novel and relevant for implementing the new antenna tuning concept. The results indicate only minor effect on efficiency, thus verifying that the multiantenna concept is applicable to modern integrated radio transceivers.

II. Antenna Cluster Efficiency

The frequency-reconfigurable antenna cluster consists of multiple antennas of different physical dimensions, placed in close proximity to take advantage of mutual coupling. The basic idea is to combine the fields generated by each antenna element in the most efficient way by properly weighting the signals to each element. For the analysis, the antenna can simply be represented by a scattering matrix. The matching efficiency of a multiport antenna with a specific excitation (later denoted as *cluster efficiency*) is [5]

$$\eta_{\mathrm{ant}} = \frac{\mathbf{a}^{\mathrm{H}}\left(\mathbf{I} - \mathbf{S}^{\mathrm{H}}\mathbf{S}\right)\mathbf{a}}{\mathbf{a}^{\mathrm{H}}\mathbf{a}} \tag{1}$$

where $(\cdot)^{\mathrm{H}}$ is the conjugate transpose, $\mathbf{I}$ is the identity matrix, an antenna is described with a scattering matrix $\mathbf{S}$, and vector

$$\mathbf{a} = \begin{bmatrix} \alpha_1 & \alpha_2 & \cdots & \alpha_n \end{bmatrix}^T P_{\mathrm{in}} \tag{2}$$

describes how the input power P_{in} is fed to the ports with different complex (amplitude and phase) coefficients α_i. The maximum cluster efficiency at a specific frequency is obtained

Manuscript received January 5, 2018; revised February 23, 2018; accepted March 6, 2018. Date of publication April 9, 2018; date of current version May 3, 2018.This work was supported in part by the Aalto ELEC Doctoral School, Academy of Finland, under Decision 289320, in part by the Nokia Foundation, in part by the Finnish Foundation for Technology Promotion, in part by the Emil Aaltonen Foundation, and in part by the KAUTE foundation. *(Corresponding author: Jari-Matti Hannula.)*

The authors are with the Department of Electronics and Nanoengineering, Aalto University School of Electrical Engineering, Espoo 02150, Finland (e-mail: jari-matti.hannula@aalto.fi; marko.kosunen@aalto.fi; anu.lehtovuori@aalto.fi; kimmor@chalmers.se; kari.stadius@aalto.fi; jussi.ryynanen@aalto.fi; ville.viikari@aalto.fi).

Digital Object Identifier 10.1109/LAWP.2018.2814059

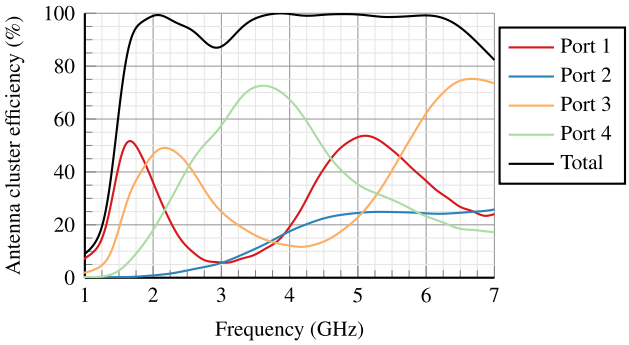

Fig. 1. Individual efficiencies of the antennas in a multiport antenna cluster [6]. The black line depicts the maximum obtainable cluster efficiency when all the antennas are used together.

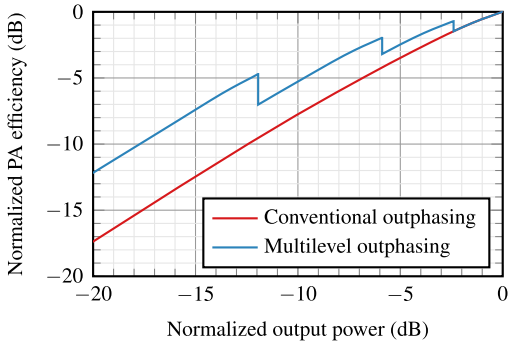

Fig. 2. Typical normalized PA back-off efficiencies of conventional and multilevel outphasing transmitters [7].

by finding the largest eigenvalue of $\mathbf{I} - \mathbf{S}^{\mathrm{H}}\mathbf{S}$ at that frequency, and then feeding the antenna with the corresponding eigenvector $\mathbf{a}$ [5].

Fig. 1 depicts the performance of the antenna cluster used in the analysis of this letter. The antenna consists of four individual antenna elements, each with a different resonant frequency. If the antennas are used individually, the efficiency is poor due to impedance mismatch and mutual coupling. However, when used together, an efficient performance can be obtained, as shown by the black curve, which represents the theoretical maximum for this specific antenna cluster with respect to a 50 Ω interface. This value is used as a reference for the results of this letter. For more details on the antenna dimensions and operation, see [6].

III. Transmitter Efficiency

The efficient operation of the antenna cluster requires that the integrated transmitter should be able to divide the signal to different antennas with varying amplitude and phase, without significant power loss. The phase tuning is not a problem, as high time resolution is in principle well supported by modern semiconductor processes. Instead, the limiting factor is amplitude tuning. Traditionally, maximum efficiency is achieved with the largest output amplitudes, and efficiency decreases with signal amplitude due to constant power consumption overhead. Several PA classes and architectures have been introduced and analyzed to improve the efficiency at lower output power [8]. Reducing the output to tune the antenna also reduces the dynamic range available for the signal. Additionally, certain modulation methods require presenting the amplitude information with sufficiently high resolution to preserve the signal integrity.

The described challenges can be alleviated by using the outphasing transmitter architecture [9], which provides several advantages. First, the information is fully coded in the phase. Transmitters relying on phase modulation are inherently suitable to be used with highly nonlinear switching PAs of high efficiency because phase-modulated signals do not suffer from harmonic distortion. Additionally, the recently proposed phase modulation methods [10]–[12] inherently support the phase tuning of multiport antenna cluster configurations targeting multi-GHz operating frequency range. Multilevel outphasing can also be used to improve the back-off efficiency [9].

Therefore, a digital multilevel outphasing transmitter has been chosen as the reference antenna driver. The efficiency optimization of the multiport antenna system is carried out using an efficiency profile of a multilevel outphasing transmitter, presented in Fig. 2.

When only the antenna is considered, finding the optimal coefficients is straightforward [5]. However, the efficiency of a PA depends on the coefficients α_i, and consequently, coefficients need to be redetermined to optimize the efficiency of the entire system. For a multioutput transmitter, the efficiency is

$$\eta_{\mathrm{amp}} = \frac{\mathbf{a}^{\mathrm{H}}\mathbf{N}\mathbf{a}}{\mathbf{a}^{\mathrm{H}}\mathbf{a}} \tag{3}$$

where

$$\mathbf{N} = \mathrm{diag}\big[\,\eta(\alpha_1) \quad \eta(\alpha_2) \quad \cdots \quad \eta(\alpha_n)\,\big] \tag{4}$$

in which $\eta(\alpha_i)$ is the efficiency of each amplifier as a function of output power. Fig. 2 illustrates a typical power–efficiency curve of an outphasing amplifier. The maximum efficiency for this kind of PA is around 30% [7], but for evaluating the performance of the antenna cluster, we only consider the reduction in efficiency due to driving the amplifier with smaller power, i.e., the efficiency at maximum power is normalized to 0 dB. We can then define the tuning efficiency, which considers both the transmitter and cluster efficiencies, as

$$\eta_{\mathrm{tot}} = \eta_{\mathrm{ant}}\eta_{\mathrm{amp}} = \frac{\mathbf{a}^{\mathrm{H}}\left(\mathbf{I} - \mathbf{S}^{\mathrm{H}}\mathbf{S}\right)\mathbf{a}}{\mathbf{a}^{\mathrm{H}}\mathbf{a}} \cdot \frac{\mathbf{a}^{\mathrm{H}}\mathbf{N}\mathbf{a}}{\mathbf{a}^{\mathrm{H}}\mathbf{a}}. \tag{5}$$

With this result, finding the optimal tuning efficiency of a multiport antenna system is now possible.

First, the system is evaluated after optimizing it only for the antenna of Fig. 1, as explained in [5]. Then, both the antenna and the transmitter are considered in the optimization by maximizing the efficiency of the system calculated from (5). For the transmitter, we assume that the PA has the efficiency profile of the multilevel outphasing transmitter depicted in Fig. 2 [7]. The power-dependent transmitter efficiency makes this a nonlinear problem, which requires nonlinear optimization methods. The optimization is performed using the trust region algorithm [13], implemented within MATLAB. Because amplitude tuning reduces the efficiency and increases the complexity of the transmitter, we also investigate a case where only the phase is tuned.

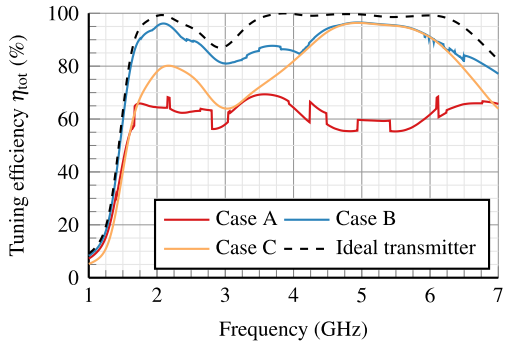

Fig. 3. Total tuning efficiency of the antenna–transmitter system in the different investigated cases.

Fig. 3 depicts the efficiency for these three different cases. Efficiency with an ideal transmitter is shown for comparison. The worst result is obtained when the weights are optimized for the antenna alone (case A). Although the antenna performance is very good in this case, the transmitter inefficiency drops the efficiency drastically. A better result is obtained by maximizing the tuning efficiency of the system (case B). In this case, the tuning efficiency is over 80% across the whole operating band. Using only phase tuning (case C) could be beneficial to simplify the transmitter, as with this approach, the efficiency exceeds that of case A. At some frequencies, the result is even comparable to case B. This occurs especially around 5 GHz, where the antenna matching is more balanced (see Fig. 1). However, the performance of this approach drops at the lower frequencies, where antenna matching levels vary more. This suggests that amplitude tuning is required for best overall performance.

In all the cases studied, the phases always converge to the same result, which was calculated analytically from (1). Consequently, the calculation of the optimal phases does not require nonlinear optimization.

IV. Receiver Architecture

Design challenges of receivers are similar to those of transmitters. The receivers must be matched at the reception bands, and the phases and amplitudes of the received signals must be tuned according to the properties of the antenna cluster. In addition, the receivers must be designed to cope with the interfering signals. In the receivers, the amplitude and phase tuning can be implemented in any part of the receiver chain similarly as in beam-steering receivers [14]. The placement of the tuning blocks is basically a tradeoff between area, power consumption, and performance.

Of the receiver properties, the input impedance is of high interest to the antenna–receiver codesign, as it can drastically change how the antenna and the receiver interact. We have considered two different receiver alternatives. The first option is a very traditional inductively degenerated low-noise amplifier (LNA). It is used to demonstrate the feasibility of the antenna system with relatively narrowband matching. The second solution is based on an N-path mixer-first receiver concept, which has gained a lot of attention in the solid-state community [1], [15]. The N-path receiver matching follows the received signal

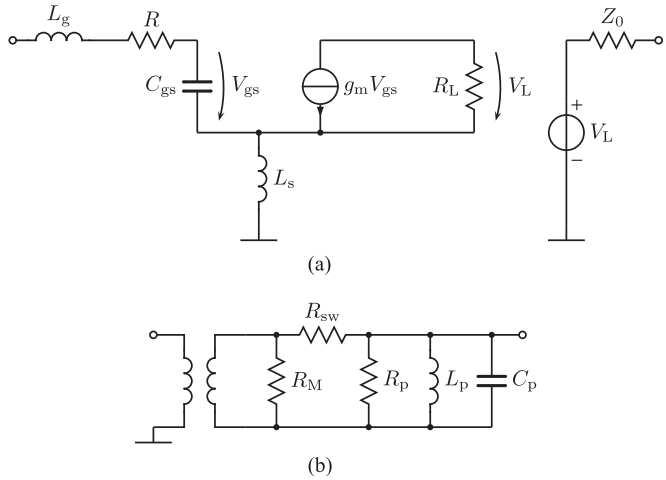

Fig. 4. Equivalent circuits for the two receiver alternatives. (a) Inductively degenerated LNA and (b) N-path mixer-first receiver.

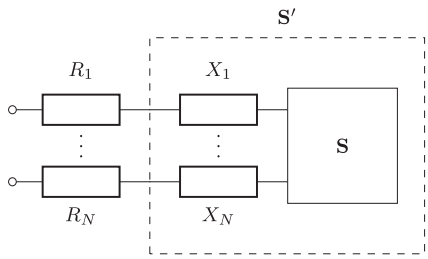

Fig. 5. Receiver input impedance can be taken into account by embedding the receiver reactance to the antenna scattering matrix $\mathbf{S}$ and renormalizing $\mathbf{S}'$ according to the receiver resistance.

frequency, and it also provides filtering already at the receiver input, which improves the receiver interference tolerance. Next, we model the receiver impedance and study its effect on total efficiency.

A. Impedance Modeling

The common assumption when matching either an antenna or a receiver is that the impedance on the other side of the interface is exactly 50 Ω. However, in the antenna cluster approach, a more thorough analysis of both impedances and their relation is needed. We describe the antenna–receiver interaction by modeling the two receiver input impedances with equivalent circuits as shown in Fig. 4.

The receiver impedance must be considered when calculating the weighting coefficients, as (1) assumes that the impedance seen by the antenna ports equals the normalization impedance of the scattering parameters. The input impedances of a receiver can be represented as the input resistance R_i and input reactance X_i. The input reactance can be de-embedded from the receiver and embedded into the antenna impedances, as illustrated in Fig. 5. The new weights can then be calculated normally from (1), after replacing $\mathbf{S}$ with $\mathbf{S}'$. Additionally, if the input resistances R_i differ from the normalization impedance Z_0, $\mathbf{S}'$ should be renormalized to match the new impedances.

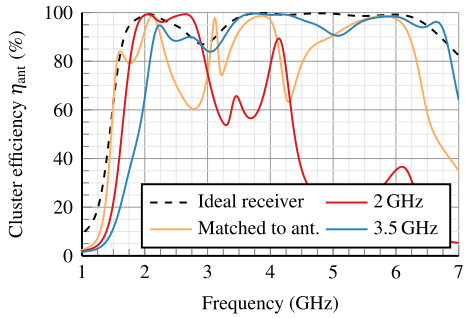

Fig. 6. Maximum obtainable cluster efficiency between the antenna and the receiver based on the inductively degenerated LNA.

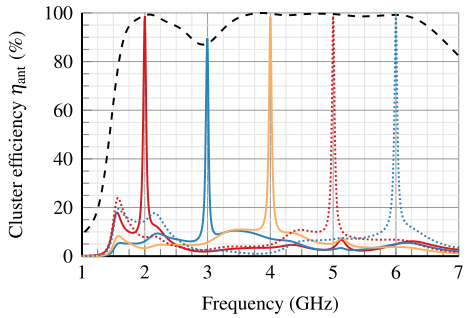

Fig. 7. Cluster efficiency with the mixer-first receiver when the system is tuned to five different frequencies, referenced against the envelope of the ideal receiver.

B. Inductively Degenerated LNA

For the inductively degenerated LNA of Fig. 4(a), three different tuning configurations are studied: all LNAs resonate at 2 GHz; they resonate at 3.5 GHz, and each LNA branch is tuned close to the resonant frequency of the corresponding antenna. As shown in Fig, 1, these are 1.5, 2, 3.5, and 6 GHz.

Fig. 6 depicts the envelope of the maximum obtainable cluster efficiency at each frequency point. The results show that the concept still works with the narrowband LNAs. However, there are some limitations caused by the limited bandwidth of the LNAs. If all LNAs resonate at 2 GHz, the upper-band performance is lost. Using LNAs designed for 3.5 GHz results in continuous tunability range, although at the expense of the lower-band performance. Designing the LNAs to match their corresponding antennas reduces the mutual coupling of the antennas, which lowers the efficiency outside the antenna resonances. However, the used model is narrowband, and more wideband receivers should be used in practice.

C. Mixer-First Receiver

The same analysis is then performed for the mixer-first receiver. The receiver is modeled using the RLC equivalent circuit in Fig. 4(b), following the procedure detailed in [16]. Fig. 7 illustrates the result when the switching frequency f_s is swept across the operating band of the antenna. The passband efficiency follows the envelope of the ideal receiver. In addition to the good passband performance, the N-path receiver also provides out-of-band isolation, which improves the interference tolerance of the receiver. This isolation is limited by the switch resistance R_{sw}. The results suggest that the mixer-first approach would be suitable for implementing the antenna cluster.

V. Conclusion

Limited size available for antennas together with increasing bandwidth requirements drive toward new antenna–transceiver systems. This letter discussed the feasibility of implementing a novel tunable antenna system when the transceiver properties are taken into account. The results indicate only a minor effect on transceiver performance and efficiency, thus verifying that the method is applicable to integrated transceivers. Based on the insights of this letter, the transceiver properties can be taken into account in future antenna cluster designs. This new paradigm of frequency-reconfigurable antennas may offer superior performance over traditional solutions, emphasizing the importance of seamless codesign of antennas and integrated transceivers.

References

[1] M. Kaltiokallio, R. Valkonen, K. Stadius, and J. Ryynänen, "A 0.7–2.7-GHz blocker-tolerant compact-size single-antenna receiver for wideband mobile applications," *IEEE Trans. Microw. Theory Techn.*, vol. 61, no. 9, pp. 3339–3349, Sep. 2013.

[2] R. Valkonen, M. Kaltiokallio, and C. Icheln, "Capacitive coupling element antennas for multi-standard mobile handsets," *IEEE Trans. Antennas Propag.*, vol. 61, no. 5, pp. 2783–2791, May 2013.

[3] P. Bahramzy *et al.*, "A tunable RF front-end with narrowband antennas for mobile devices," *IEEE Trans. Microw. Theory Techn.*, vol. 63, no. 10, pp. 3300–3310, Oct. 2015.

[4] M. Stoopman, Y. Liu, H. J. Visser, K. Philips, and W. A. Serdijn, "Codesign of electrically short antenna–electronics interfaces in the receiving mode," *IEEE Trans. Circuits Syst. II*, vol. 62, no. 7, pp. 711–715, Jul. 2015.

[5] J.-M. Hannula, J. Holopainen, and V. Viikari, "Concept for frequency reconfigurable antenna based on distributed transceivers," *IEEE Antennas Wireless Propag. Lett.*, vol. 16, pp. 764–767, 2017.

[6] J.-M. Hannula, T. Saarinen, J. Holopainen, and V. Viikari, "Frequency reconfigurable multiband handset antenna based on a multichannel transceiver," *IEEE Trans. Antennas Propag.*, vol. 65, no. 9, pp. 4452–4460, Sep. 2017.

[7] M. Martelius *et al.*, "Class D CMOS power amplifier with on/off logic for a multilevel outphasing transmitter," in *Proc. IEEE Int. Symp. Circuits Syst.*, May 2016, pp. 710–713.

[8] T. Johansson and J. Fritzin, "A review of watt-level CMOS RF power amplifiers," *IEEE Trans. Microw. Theory Techn.*, vol. 62, no. 1, pp. 111–124, Jan. 2014.

[9] P. Godoy, S. Chung, T. Barton, D. Perreault, and J. Dawson, "A 2.4-GHz, 27-dBm asymmetric multilevel outphasing power amplifier in 65-nm CMOS," *IEEE J. Solid-State Circuits*, vol. 47, no. 10, pp. 2372–2384, Oct. 2012.

[10] D. Seebacher *et al.*, "Reduction of aliasing effects of RF PWM modulated signals by cross point estimation," *IEEE Trans. Circuits Syst. I*, vol. 61, no. 11, pp. 3184–3192, Nov. 2014.

[11] J. Lemberg *et al.*, "Digital interpolating phase modulator for wideband outphasing transmitters," *IEEE Trans. Circuits Syst. I*, vol. 63, no. 5, pp. 705–715, May 2016.

[12] M. Kosunen *et al.*, "A 0.35-to-2.6GHz multilevel outphasing transmitter with a digital interpolating phase modulator enabling up to 400 MHz instantaneous bandwidth," in *Proc. IEEE Int. Solid-State Circuits Conf. Dig. Tech. Papers*, 2017, pp. 224–225.

[13] J. J. Moré and D. C. Sorensen, "Computing a trust region step," *SIAM J. Sci. Comput.*, vol. 4, no. 3, pp. 553–572, 1983.

[14] A. Natarajan *et al.*, "A fully-integrated 16-element phased-array receiver in SiGe BiCMOS for 60-GHz communications," *IEEE J. Solid-State Circuits*, vol. 46, no. 5, pp. 1059–1075, May 2011.

[15] H. Darabi, A. Mirzaei, and M. Mikhemar, "Highly integrated and tunable RF front ends for reconfigurable multiband transceivers: A tutorial," *IEEE Trans. Circuits Syst. I*, vol. 58, no. 9, pp. 2038–2050, Sep. 2011.

[16] A. Ghaffari, E. A. M. Klumperink, M. C. M. Soer, and B. Nauta, "Tunable high-Q N-path band-pass filters: Modeling and verification," *IEEE J. Solid-State Circuits*, vol. 46, no. 5, pp. 998–1010, May 2011.